Research Paper

PAIN®

OPEN

OnabotulinumtoxinA affects cortical recovery period but not occurrence or propagation of cortical spreading depression in rats with compromised blood–brain barrier

Agustin Melo-Carrillo[a,b], Andrew M. Strassman[a,b], Aaron J. Schain[a,b], Ron S. Broide[c], Brian B. Cai[c], Catherine Rhéaume[c], Amy D. Brideau-Andersen[c], Sait Ashina[a,b], Yadira Flores-Montanez[a,b], Mitchell F. Brin[c,d], Rami Burstein[a,b,*]

Abstract

OnabotulinumtoxinA (BoNT-A) is an Food and Drug Administration-approved, peripherally acting preventive migraine drug capable of inhibiting meningeal nociceptors. Expanding our view of how else this neurotoxin attenuates the activation of the meningeal nociceptors, we reasoned that if the stimulus that triggers the activation of the nociceptor is lessened, the magnitude and/or duration of the nociceptors' activation could diminish as well. In the current study, we further examine this possibility using electrocorticogram recording techniques, immunohistochemistry, and 2-photon microscopy. We report (1) that scalp (head) but not lumbar (back) injections of BoNT-A shorten the period of profound depression of spontaneous cortical activity that follows a pinprick-induced cortical spreading depression (CSD); (2) that neither scalp nor lumbar injections prevent the induction, occurrence, propagation, or spreading velocity of a single wave of CSD; (3) that cleaved SNAP25—one of the most convincing tools to determine the anatomical targeting of BoNT-A treatment—could easily be detected in pericranial muscles at the injection sites and in nerve fibers of the intracranial dura, but not within any cortical area affected by the CSD; (4) that the absence of cleaved SNAP25 within the cortex and pia is unrelated to whether the blood–brain barrier is intact or compromised; and (5) that BoNT-A does not alter vascular responses to CSD. To the best of our knowledge, this is the first report of peripherally applied BoNT-A's ability to alter a neuronal function along a central nervous system pathway involved in the pathophysiology of migraine.

Keywords: Migraine, Headache, Trigeminal, Aura, Botox, Calcitonin gene-related peptide, Trigeminovascular

1. Introduction

Migraine with aura is a highly prevalent disorder affecting approximately 5% of the general population.[42] It is defined as a transient neurological disturbance in visual or sensory perception and speech production[49,50] that most commonly appears shortly before and less commonly at the onset of the headache phase of an attack.[17,23] Evidence from human imaging studies[10,16,46] has given support to the idea, originally proposed by Milner,[36] that the physiological substrate of the migraine aura is cortical spreading depression (CSD), a cortical phenomenon characterized by a slowly propagating wave of brief neuronal depolarization, followed by more prolonged inhibition.[27,28] Consequently, CSD has become one of the most commonly used and best characterized animal models of migraine.[5,9,23,24,40]

Previous studies have demonstrated that CSD is capable of activating peripheral[52] and central[51] neurons of the meningeal sensory pathway, which is thought to be critically involved in initiating the headache phase of migraine.[37] Examining the notion that the headache phase of migraine begins with the activation of meningeal nociceptors, in the past few years, we showed that common peripherally and centrally acting acute migraine drugs (eg, triptans and nonsteroidal anti-inflammatory drugs),[6,19,20,29,30] as well as peripherally acting prophylactic migraine drugs (eg, onabotulinymtoxinA and anti-calcitonin gene-related peptide [CGRP] monoclonal antibodies)[7,31,33,34,53] attenuate the activation of peripheral and central trigeminovascular neurons and proposed that these modulatory actions explain in part how these drugs terminate or prevent the headache phase of migraine. But as is the case with almost all drugs (eg, statins), the likelihood that these migraine drugs achieve their therapeutic effects through one and only one mechanism is slim and improbable.

Expanding our view of how else antimigraine drugs can attenuate the activation of the meningeal nociceptors, we reasoned that if the stimulus that triggers the activation of the nociceptor is lessened, the magnitude and/or duration of the

Sponsorships or competing interests that may be relevant to content are disclosed at the end of this article.

[a] Department of Anesthesia, Critical Care and Pain Medicine, Beth Israel Deaconess Medical Center, Boston MA, United States, [b] Department of Anesthesia, Harvard Medical School, Boston MA, United States, [c] Allergan, an AbbVie Company, Irvine, CA, United States, [d] University of California, Irvine, United States

**Corresponding author. Address: Department of Anesthesia, Critical Care and Pain Medicine, Beth Israel Deaconess Medical Center, CLS-649, 3 Blackfan Circle, Boston, MA 02215, United States. Tel.: 617-735-2832; fax: 617-735-2833. E-mail address: rburstei@bidmc.harvard.edu (R. Burstein).*

PAIN 162 (2021) 2418–2427

http://dx.doi.org/10.1097/j.pain.0000000000002230

nociceptors' activation could diminish as well. Along this line, we reported recently that intravenous administration of fremanezumab, a humanized anti-CGRP monoclonal antibody (anti-CGRP-mAb) that is too large to cross the blood–brain barrier (BBB), alters some of the properties of CSD.[32] The unexpected findings of that study raised the possibility that onabotulinumtoxinA (BoNT-A), another peripherally acting migraine prophylactic drug that is too large to cross the BBB and act centrally, can also alter the physiological properties of CSD. OnabotulinumtoxinA is an Food and Drug Administration-approved migraine prophylactic drug[2,12] capable of inhibiting activation of unmyelinated C- but not thinly myelinated Aδ-meningeal nociceptor responses to CSD,[34] TRPV1 and TRPA1 agonists,[53] and administration of inflammatory mediators to their dural receptive fields.[7]

In the current study, we measured BoNT-A effects on amplitude and propagation rate of CSD, on the cortical silencing period that follows the CSD, and on responses of pial and dural arteries and veins to CSD after scalp and lumbar injections. Because the method we used to induce CSD causes local disruption of the BBB, we also investigated the presence of BoNT/A-cleaved SNAP25 ($SNAP25_{197}$) in cortical areas involved in the propagation of CSD.

2. Materials and methods

Experiments were approved by the Beth Israel Deaconess Medical Center and Harvard Medical School standing committees on animal care and were conducted in accordance with the U.S. National Institutes of Health's *Guide for the Care and Use of Laboratory Animals*.

2.1. OnabotulinumtoxinA injections

Seven days before surgical preparation, male and female Sprague-Dawley rats (250-300 g) were briefly anesthetized (2% isoflurane) and injected with BoNT-A (final dose = 1 unit) or vehicle (normal saline). Five injections of BoNT-A (each containing 0.20 units diluted in 1 μL of saline) or saline (5 μL) were made in the scalp along the lambdoid and sagittal sutures (2 injections on each side and one in the middle) as described before (Zhang, 2016) (**Fig. 1A**). In a separate group of animals, 5 subcutaneous injections of BoNT-A (each containing 0.20 units diluted in 1 μL of saline) were made in the lower back of the rat (**Fig. 1B**), to compare with those animals injected in the head.

2.2. Rationale for using 1 unit

We chose 1 unit (about 3-4 units/kg for 250-300 g rats) because (1) the results it produced were similar to the results produced with higher doses in the pilot phase of the study, (2) it is well within the range of doses (1-10 units/kg) used in preclinical studies of small animals with fast metabolic rates,[7,8,53] and (3) it is approximately twice the dose used in clinical practice where migraine patients typically receive 2.2 units/kg (155 units given to a 70 kg person).

2.3. Surgical preparation

Seven days after BoNT-A injections, rats were anesthetized with urethane (0.9-1.2 g/kg i.p.), fitted with an endotracheal tube to allow artificial ventilation (0.1 L/min O_2) and an intrafemoral vein cannula for later infusion of fluids. Rats were placed in a stereotaxic apparatus, and core temperature was kept at 37°C using a heating blanket. End-tidal CO_2 was monitored continuously and kept within physiological range (3.5-4.5 pCO_2). Once stabilized, rats received a continuous infusion of 0.9% saline at a rate of 1.0 mL/hour. For placing the electrocorticogram electrodes, a large craniotomy (6 × 6 mm) was performed between lambda and bregma, and the exposed dura was kept covered and moist.

2.4. Cortical spreading depression induction and electrocorticogram recording

We induced CSD in the occipital cortex by pinprick and recorded its propagation using 2 glass micropipettes (7 μm tip, ~1 MΩ, filled with 0.9% saline, at a depth of ~100 μm), one placed in the occipital cortex and the second, 4 mm anteriorly within the parietal cortex. This configuration allowed us to measure the amplitude, recovery period, and spreading velocity of each wave of CSD (**Fig. 2**). Using Spike2 software (CED), the electrocorticogram was captured and filtered offline in 2 different ways to allow accurate measurements of the different parameters. A partial DC removal filter (time constant of 30 seconds) was used to measure CSD amplitude and the propagation velocity, whereas a full DC removal filter (time constant of 0.07 seconds) was used to measure the neuronal silencing period—defined here as the recovery period.

2.5. Experimental protocol

All experiments included continuous recording of cortical activity for 30 minutes before induction of a single wave of CSD (baseline period) and 30 minutes after the CSD wave was recorded in both the occipital and parietal cortices.

2.6. Data analyses

Included in the data analyses were CSD amplitude (defined as the peak-to-peak positive-to-negative DC shift expressed in millivolt), CSD spreading velocity (calculated as the time between the appearance of the CSD wave at the occipital and parietal electrodes divided by the distance between them and expressed in millimeter per minute), and the neuronal silencing (recovery) period (representing the depression phase of CSD) that followed the CSD wave (measured between the last signal of cortical activity at the onset of CSD and the first signal of cortical activity after the CSD wave had passed the recording electrode and expressed in seconds). The experimental set up (**Fig. 2**) allowed us to calculate one value for spreading velocity and 2 values for CSD amplitude and recovery (one measured by the occipital electrode and a second one in the parietal electrode) period per rat. Median values calculated in each of the 3 experimental groups were compared using nonparametric statistics (Kruskal–Wallis and one-way analysis of variance [ANOVA]) and post hoc analysis (Mann–Whitney). The level of significance was set at 0.05. Results are expressed as median (interquartile range [IQR]).

2.7. Anatomical experiments

Given that the animal model we used causes localized breakage of the BBB in a highly restricted area of the cortex along the path of the 2 CSD recording electrodes as well as the path of the pinprick,[39] 2 sets of experiments were performed to test the possibility that BoNT/A may have reached structures in the central nervous system (CNS) after receiving 8 extracranial injections (3 along suture lines, 2 in the temporal muscle, and 3 in neck muscles, 0.625 units per injection, as explained in Zhang et al.[53]) of toxin. This was performed by examining the immunostaining for BoNT/A-cleaved SNAP25

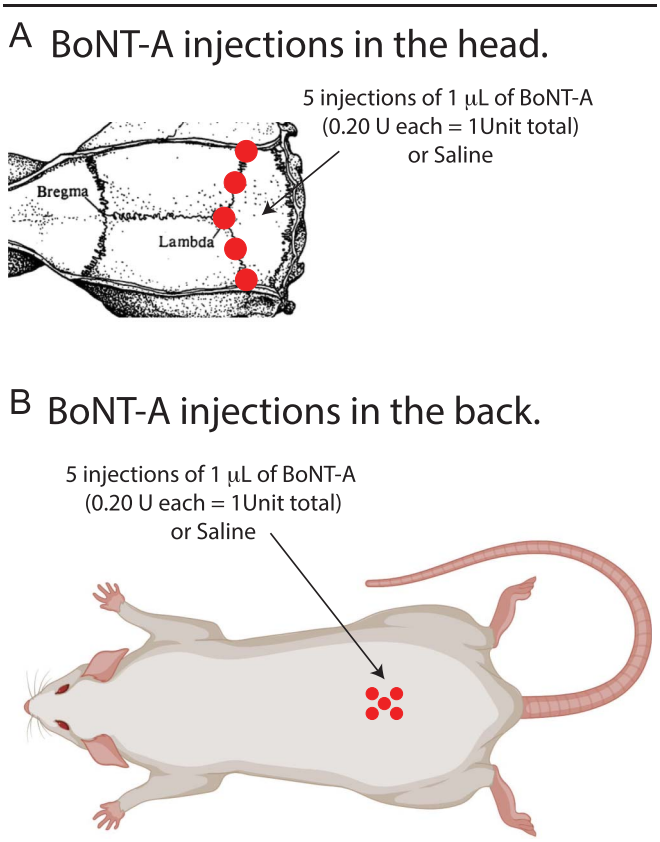

Figure 1. Scalp/suture-line and lumbar injection sites of BoNT-A. (A) Locations of the 5 injections (0.2 units each, diluted in 1 μL, total = 1 unit) made across the lambdoid and sagittal sutures. (B) Locations of the 5 injections (0.2 units each, diluted in 1 μL, total = 1 unit) made in the lumbar region. BoNT-A, onabotulinumtoxinA (created with BioRender.com).

($SNAP25_{197}$) using a highly selective antibody for the cleaved epitope (Rheaume et al., 2015). In the first set (with noncompromised BBB), rats that received extracranial BoNT-A injections 7 days earlier were anesthetized and transcardially perfused, first with 500 mL of saline/heparin, followed by 400 mL of Zamboni fixative. Rat tissues were harvested and postfixed in Zamboni fixative for 2 hours. After this, all tissue samples were immersed in 30% sucrose for 48 hours and optimal cutting temperature compound embedded at −20°C. Temporal muscle and brain were cryostat sectioned into 12-μm thick sections and air dried. Rat dura membranes were stained as whole-mounts. In the second set (with compromised BBB), rats that received extracranial injections 7 days earlier were anesthetized, but before being sacrificed, 2 craniotomies were performed and recording electrodes were placed in the parietal and occipital cortices for several hours. Finally, to test our ability to detect the presence of BoNT-A (ie, $SNAP25_{197}$ immunostaining) in the CNS structures, rats were injected with a saturating dose of BoNT-A (20 μL, 30 U/kg) intramuscularly (IM) into the midbelly of the right tibialis anterior (TA) muscle. Seven days postinjection, rats were anesthetized and transcardially perfused with the same protocol mentioned above. Spinal cord sections from L3 to L5 segments were harvested and postfixed in 4% paraformaldehyde for 2 hours. After this, tissue samples were immersed in 30% sucrose for 48 hours and optimal cutting temperature compound embedded at −20°C. Spinal cord sections were cryostat sectioned into 12-μm thick sections and air dried.

2.8. Antibodies

The following primary antibodies were used in this study: recombinant human anti-$SNAP25_{197}$ (Ab632) rMAb (Allergan, Inc, Irvine, CA[44]) and rabbit anti-SNAP25 monoclonal antibody (Epitomics-Abcam, Cambridge, MA). The following secondary antibodies were used in this study: donkey anti-human immunoglobulin G (IgG) Alexa Fluor 488 (709-545-149) and donkey anti-rabbit IgG Alexa Fluor 594 (Jackson Immuno Research, West Grove, PA). α-Bungarotoxin, Alexa Fluor 488, conjugate was purchased from Invitrogen Life Technologies (Carlsbad, CA).

2.9. Immunohistochemistry

Slide-mounted sections were incubated in blocking buffer (1X phosphate buffered saline + 5% normal donkey derum+ 0.1% Triton X-100) to prevent nonspecific signal for 1 hour and then incubated with primary antibodies ($SNAP25_{197}$ at 1 μg/mL, rabbit anti-SNAP25 monoclonal antibody at 1:500) in blocking buffer overnight at 4°C. After several washes, sections were incubated

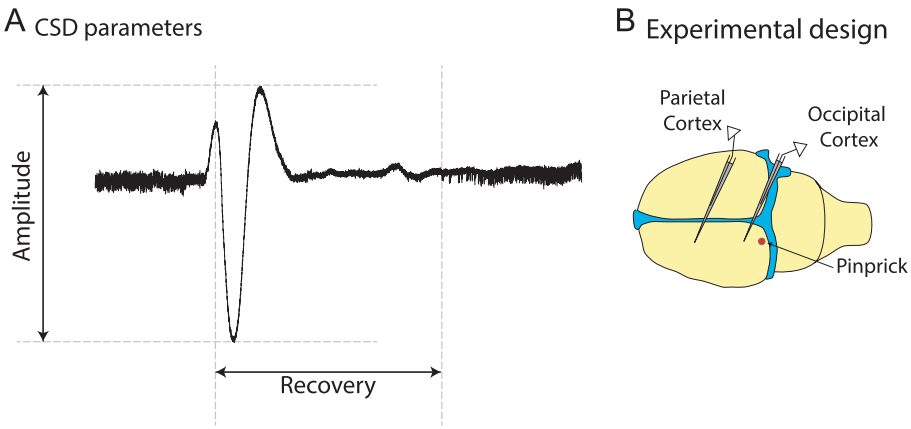

Figure 2. Recording setup and CSD characterization. (A) Schematic representation of the rat's brain showing location of recording electrodes and site of CSD induction by pinprick. (B) Cortical spreading depression trace illustrating the parameters measured for the study. Amplitude is defined as the peak-to-peak positive-to-negative direct current shift expressed in mV. Spreading velocity is calculated as the time between the appearance of the CSD wave at the occipital and parietal electrodes divided by the distance between them and expressed in millimeter per minute. Neuronal silencing period is measured between the last signal of cortical activity at the onset of CSD and the first signal of cortical activity after the CSD wave had passed the recording electrode and expressed in seconds. CSD, cortical spreading depression.

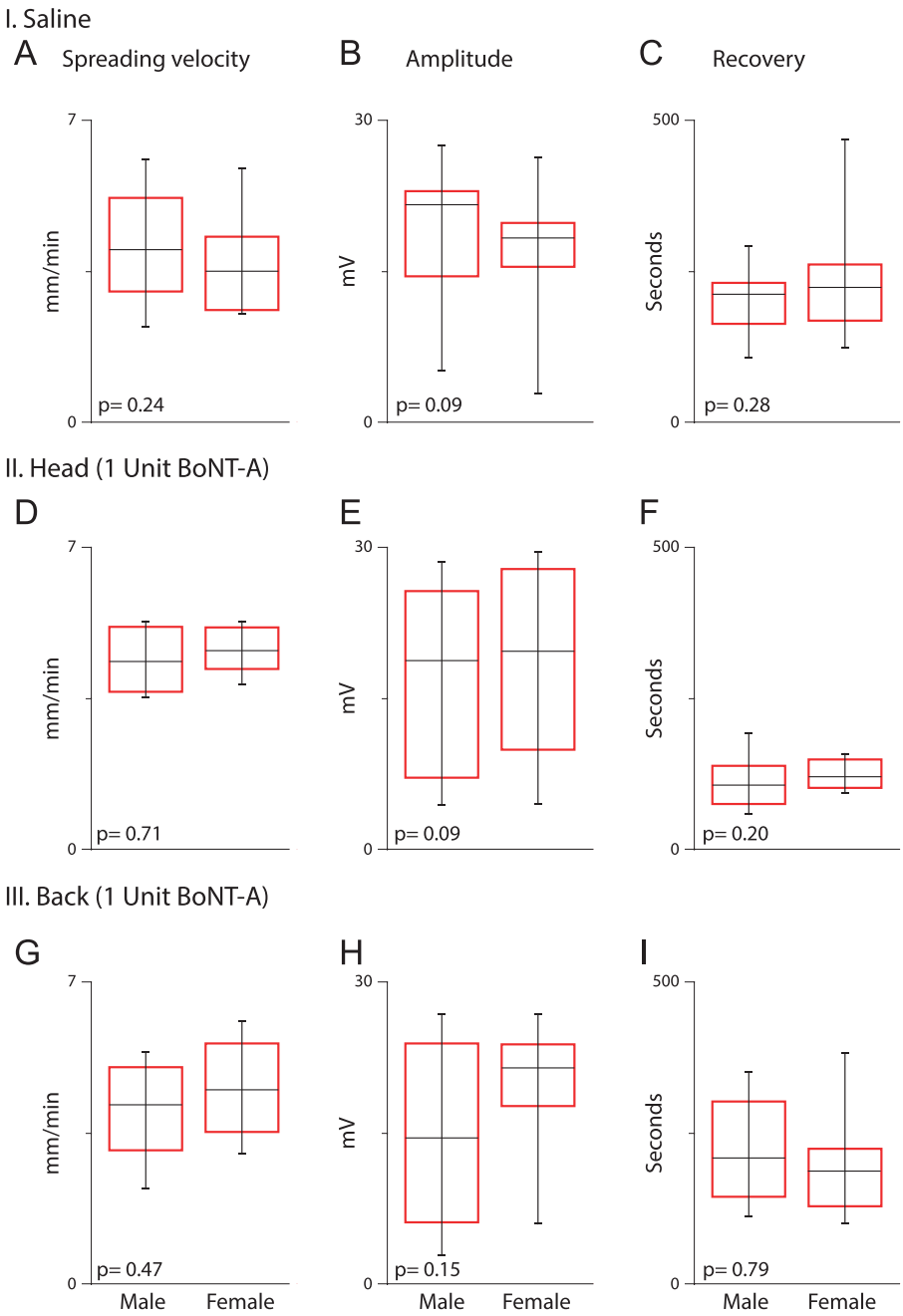

Figure 3. Effects of saline (I) and BoNT-A (II III) injections on CSD parameters in male vs female rats. Box plots (median and IQR) of spreading velocity (A, D, G), amplitude (B, E, H), and recovery (C, F, I) showing no differences in any of the measured CSD parameters in male vs female rats. BoNT-A, onabotulinumtoxinA; CSD, cortical spreading depression; IQR, interquartile range.

with Alexa Fluor–labeled secondary antibodies (donkey anti-human IgG Alexa Fluor 488 and donkey anti-rabbit IgG Alexa Fluor 594) diluted (1:1000) in blocking buffer for 2 hours at room temperature and then washed again. Slide-mounted sections were coverslipped using ProLong Gold Antifade mounting media with DAPI (Life Technologies, Grand Island, NY). Dura whole-mounts were transferred into a 12-well culture plate paired with a 15-mm Netwell insert and incubated in blocking buffer (1X phosphate buffered saline + 10% normal donkey serum + 0.1% Triton X-100) to prevent nonspecific signal for 1 hour at room temperature with agitation. The dura whole-mounts were then incubated with primary antibodies (human anti-$SNAP25_{197}$ at 0.8 μg/mL) in blocking buffer for 48 hours at 4°C with agitation. After several washes, the tissue was incubated with Alexa Fluor–labeled secondary antibodies (donkey anti-human IgG Alexa Fluor 488; 1:100) diluted in blocking buffer for 2 hours at room temperature and then washed again. Dura whole-mounts were slide-mounted and cover slipped using Fluoromount-G (EM Sciences, Hatfield, PA) containing 1.5 μg/mL DAPI (Roche Diagnostics, Indianapolis, IN) to label cellular nuclei.

2.10. Image acquisition

Muscle, brain, and spinal cord stack images were acquired using an Olympus FV1200 confocal microscope (Olympus, Waltham, MA) with Olympus FluoView FV-10 ASW software

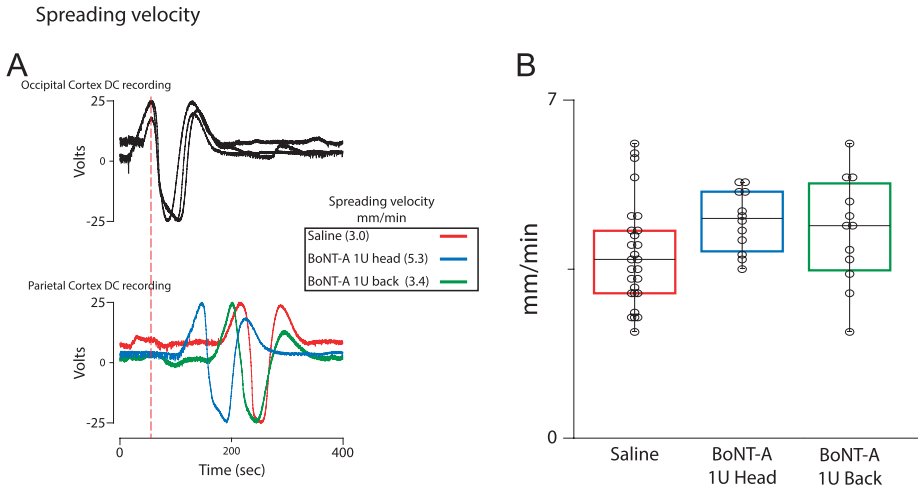

Figure 4. Spreading velocity. (A) Electrocorticogram traces showing rates of CSD spreading velocities in rats injected with saline or BoNT-A in the scalp/suture lines and rats injected with BoNT-A in the back. (B) Box plots (median and IQR) showing no differences in the CSD spreading velocity between the 3 groups of rats ($P = 0.058$). (CSD spreading velocity was 3.7 mm/min (IQR: 3.0-4.3) in the control group (n = 27), 4.5 mm/min (IQR: 3.8-5.1) in the animals injected with BoNT-A in the head (n = 12), and 4.4 mm/min (IQR: 3.4-5.2) in the animals injected with BoNT-A in the back (n = 12). There was no significant difference between the animals injected with BoNT-A in the head and back ($P = 0.707$). BoNT-A, onabotulinumtoxinA; CSD, cortical spreading depression.

using 30x and 40x oil objectives. Dura whole-mount stack images were captured using a Zeiss LSM-710 confocal microscope (Carl Zeiss, Thornwood, NY) with Zeiss ZEN software (version 5.5, Carl Zeiss, 2009) using 20x and 40x oil objectives. The resulting 3D images were analyzed using Imaris software (Bitplane, Concord, MA).

2.11. Vascular imaging of rats

Rats were injected with BoNT-A or with saline as described above 1 week before imaging. On the day of imaging, rats were anesthetized using 1.5 g/kg urethane and 3 mL of atropine and prepared for imaging and imaged as previously described (Schain 2019). In brief, rats had a femoral artery cannula inserted, were placed in a stereotax, the scalp was retracted, and the parietal skull bone was thinned until transparent. On the frontal skull plate, a small craniotomy was made for the placement of the CSD-inducing electrode. Rats were then placed in a 2-photon microscope (Olympus FV-1000), and an image was taken at 800 nm excitation, which reveals arterial smooth muscle and aids in the selection of a location with a dural artery, dural vein, pial artery, and pial vein all within view. Rats were then injected intravenously with 2 MDa fluorescein isothiocyanate-dextran to label blood plasma. Rats were then imaged repeatedly at an excitation of 890 nm with 6 image slices, 3 in the dura and 3 in the pia approximately 10 μm apart, which takes about 10 seconds to image the entire stack. Images were taken for 2 minutes from baseline; after which CSD was induced, and then images were taken for at least another 20 minutes. Vessel diameter was quantified at every time point using Fiji image analysis software (http://www.fiji.sc) and a custom written macro.

2.12. Statistical analysis

Two-tailed *t* test was used to compare means unless otherwise noted. Two rats were excluded from the data because they were outliers from a normal distribution of dura dilation post-CSD, one in the control group and one in the BoNT-A group. For all of the vascular data, we used n = 10 animals per treatment group.

3. Results

One hundred two rats were used in the 2 phases of this study. In the first phase, 24 males and 27 females rats were studied 7, 8, 9, 10, or 11 days after receiving saline (6 males and 9 females) or BoNT-A (6 males and 6 females) injections in the head, or saline (6 males and 6 females) or BoNT-A (6 males and 6 females) injections in back. Data obtained in this phase of the study were not included in the analysis as they seemed to be affected by the number of days postinjections. In the second phase, 27 male and 24 female rats were studied exactly 7 days after receiving saline (9 males and 6 females) or 1 unit of BoNT-A (6 males and 6 females) injections in the head, or saline (6 males and 6 females) or 1 unit of BoNT-A (6 males and 6 females) injections in back.

3.1. Cortical spreading depression parameters in saline- and BoNT-A-injected female and male rats are similar

In rats injected with saline (**Figs. 3A–C**), spreading velocity (calculated based on 15 CSDs in males and 12 CSDs in females) was 4.0 mm/minute (IQR: 3.03-5.2) in males and 3.5 mm/min (IQR: 2.6-4.3) in females ($P = 0.240$ [$U = 65.5$, $n_1 = 12$, $n_2 = 15$, Mann–Whitney]) (**Fig. 3**). Cortical spreading depression amplitude was 21.5 mV (IQR: 14.4-22.9) in males (n = 30 CSDs) and 18.2 mV (IQR: 15.4-19.7) in females (n = 24 CSDs, $P = 0.098$ [$U = 264.5$, $n_1 = 24$, $n_2 = 30$, Mann–Whitney]). Neuronal silencing (recovery) period was 211.8 seconds (IQR: 162.8-230.7) in males (n = 30 CSDs) and 223.1 second (IQR: 168.1-260.8) in females (n = 24 CSDs, $P = 0.288$ [$U = 298.5$, $n_1 = 24$, $n_2 = 30$, Mann–Whitney]). In rats injected with 1 unit BoNT-A in the head (**Figs. 3D–F**), spreading velocity (calculated based on 6 CSDs in males and 6 CSDs in females) was 4.3 mm/min (IQR: 3.65-5.15) in males and 4.6 mm/min (IQR: 4.1-5.15) in females ($P = 0.71$ [$Z = 0.42$, $n_1 = 6$, $n_2 = 6$, Wilcoxon signed-rank test]). Cortical spreading depression amplitude was 18.7 mV (IQR: 7.09-25.72) in males (n = 12 CSDs) and 19.66 mV (IQR: 9.86-27.8) in females (n = 12 CSDs, $P = 0.098$ [$Z = 3.05$, $n_1 = 12$, $n_2 = 12$, Wilcoxon signed-rank test]). Neuronal silencing (recovery) period was 105.61 seconds (IQR: 75.47-138.24) in males (n = 12 CSDs) and 119.56 seconds (IQR: 101.13-148.45) in females (n = 12 CSDs, $P = 0.203$ [$Z = 1.33$, n_1

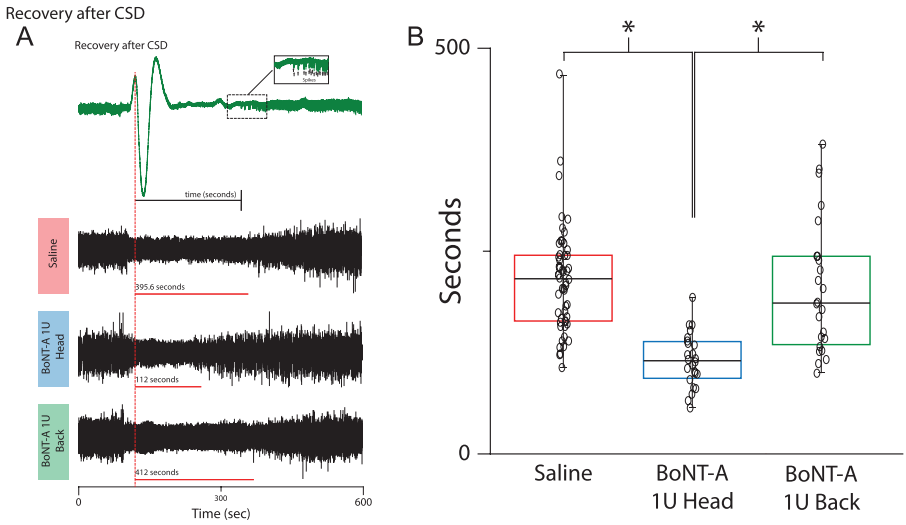

Figure 5. Cortical spreading depression–induced depression of spontaneous and evoked cortical activity. (A) Examples of electrocorticogram recording of neuronal silencing periods that follow CSD in rats injected with saline or BoNT-A in the scalp/suture lines and rats injected with BoNT-A in the back. (B) Box plot showing difference in the neuronal silencing period between the 3 groups. Note that the neuronal silencing period was significantly shorter in the group that received BoNT-A injections in the scalp/suture line than the group injected with saline ($P = 7.7 \times 10^{-10}$) in the head or BoNT-A in the back ($P = 2.2 \times 10^{-5}$). BoNT-A, onabotulinumtoxinA; CSD, cortical spreading depression.

= 12, n_2 = 12, Wilcoxon signed-rank test]). In rats injected with 1 unit BoNT-A in the back (**Figs. 3G–I**), spreading velocity (calculated based on 6 CSDs in males and 6 CSDs in females) was 4.15 mm/min (IQR: 3.1-5.02) in males and 4.5 mm/min (IQR: 3.52-5.57) in females (P= 0.47 [Z = 2.20, n_1 = 6, n_2 = 6, Wilcoxon signed-rank test]). Cortical spreading depression amplitude was 14.49 mV (IQR: 6.13-23.89) in males (n = 12 CSDs) and 21.44 mV (IQR: 17.67-23.80) in females (n = 12 CSDs, P = 0.151 [Z = 1.49, n_1 = 12, n_2 = 12, Wilcoxon signed-rank test]). Neuronal silencing (recovery) period was 208.74 seconds (IQR: 144.47-302.15) in males (n = 12 CSDs) and 186.32 seconds (IQR: 128.77-223.93) in females (n = 12 CSDs, P = 0.791 [Z = 0.313, n_1 = 12, n_2 = 12, Wilcoxon signed-rank test]). Accordingly, data obtained from the female and male rats were combined.

3.2. The propagation rate of cortical spreading depression (spreading velocity) is unaffected by injections of onabotulinumtoxinA in the head or in the back

The velocity at which CSD spread was 3.7 mm/min (IQR: 3.0-4.3) in the control group (n = 27 CSDs), 4.5 mm/min (IQR: 3.8-5.1) in animals injected with BoNT-A in the head (n = 12 CSDs), and 4.4 mm/min (IQR: 3.4-5.2) in the animals injected with BoNT-A in the back (n = 12 CSDs) (**Fig. 4**). These values yielded no significant difference between the 3 groups (χ^2 = 5.6, df = 2, P = 0.058, Kruskal–Wallis).

3.3. The cortical recovery period (period of neuronal silencing) that follows cortical spreading depression is shorter in animals injected with onabotulinumtoxinA in the head but not in the back

The neuronal silencing period induced by CSD lasted 216.3 seconds (IQR: 164.1-245.3) in the control group (n = 54 CSDs), 115 seconds (IQR: 93.4-138.7) in animals injected with BoNT-A in the head (n = 24 CSDs), and 186.3 seconds (IQR: 135.0-244.1) in the animals injected with BoNT-A in the back (n = 24 CSDs) (**Fig. 5**). These values yielded significant differences between the 3 groups (χ^2 = 38.2, df = 2, $P = 4.8 \times 10^{-9}$, Kruskal–Wallis). Furthermore, the group that received BoNT-A injections in the head differ significantly from the group that received saline injections in the head and back ($P = 7.7 \times 10^{-10}$ Mann–Whitney) as well as the group that received BoNT-A injections in the back ($P = 2.2 \times 10^{-5}$, whereas the latter 2 did not differ [P = 0.357] **Fig 5B**).

3.4. Cortical spreading depression amplitude is unaffected by onabotulinumtoxinA injections in the head or in the back

Cortical spreading depression amplitude was 18.7 mV (IQR: 15.4-22.3) in the control group (n = 54 CSDs), 19.5 mV (IQR: 9.2-25.7) in animals injected with BoNT-A in the head (n = 24 CSDs), and 20.5 mV (IQR: 10.4-23.8) in animals injected with BoNT-A in the back (n = 24 CSDs) (**Fig. 6**). These values yielded no significant difference between the 3 groups (χ^2 = 0.13, df = 2, P = 0.93, Kruskal–Wallis).

3.5. Cleaved SNAP25 is found in the dura and onabotulinumtoxinA-injected muscles after scalp injections but not in the cortex

High-resolution confocal microscopy yielded evidence for the presence of cleaved SNAP25 in a subset of nerve fibers within the temporal muscle and dura (**Fig. 7A**) of rats injected with BoNT-A 7 days earlier, but not in their cortices (**Fig. 7B**). Although *noncleaved* SNAP25 ($SNAP25_{206}$) was readily detected in the cortex (**Fig. 7B**, panel I), *cleaved* SNAP25 ($SNAP25_{197}$) could not be detected in naive and BoNT-A-injected rats with intact BBB as well as in rats in which the BBB was compromised by insertion of recording electrodes into the visual and parietal cortices and a pinprick electrode in the visual cortex (**Fig. 7B**, panels II-IV). Presence of cleaved and noncleaved $SNAP25_{197}$ in ipsilateral spinal cord ventral horn motor neurons, after BoNT/A injection into the TA muscle (**Fig. 7C**) provides evidence for our technical ability to detect these biomarkers in the CNS.[8] Of note, the presence of cleaved SNAP25 in the ventral horn was confined to

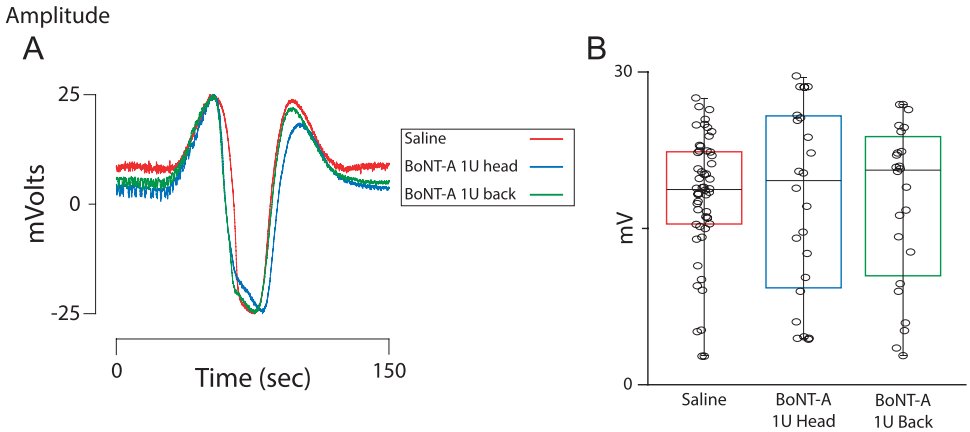

Figure 6. (A) Amplitude. Electrocorticogram traces showing CSD amplitudes in rats injected with saline or BoNT-A in the scalp/suture lines and rats injected with BoNT-A in the back. (B) Box plot showing no differences in the amplitude of the CSD wave between the saline treated group and animals injected with BoNT-A in the head and in the back ($P = 0.93$). BoNT-A, onabotulinumtoxinA; CSD, cortical spreading depression.

motor neurons in the TA-innervating region (lamina IX) of the spinal cord and was mainly observed after higher doses of BoNT/A injections (eg, 10, 30 U/kg) into the TA muscle.

3.6. Pretreatment with onabotulinumtoxinA injection in the scalp does not alter vascular response to cortical spreading depression

Pretreatment with BoNT-A had no significant effect on responses of pial or dural arteries and veins to CSD (**Fig. 8**). Pial arteries dilated within 40 seconds to a maximum increase of 42.9% ± 3.3 in the saline group and 43.0% ± 1.7 in the BoNT-A group (not significantly different, $P = 0.98$), for a duration of 82.0 seconds ± 6.5 (saline) and 93.7 seconds ± 6.9 (BoNT-A) ($P = 0.23$), and then, compared with their original diameter, constricted about 6.97% ± 1.8 in the saline group and 6.56% ± 1.5 in the BoNT-A group ($P = 0.87$) (**Fig. 8A**). For pial arteries, the area under the curve was not significantly different (13.4 ± 0.22 for saline and 13.7 ± 0.21 for BoNT-A, $P = 0.28$). There was no significant interaction between treatment group and time post-CSD according to a two-way ANOVA ($F_{(44,1)} = 0.85$, $P = 0.74$).

Dural arteries began dilating at about the same time (saline group: 148 ± 35 seconds, BoNT-A group: 115 ± 31 seconds, not significantly different between treatment groups, $P = 0.48$) and reached a similar maximum dilation (an increase of 30.0% ± 2.2 in the saline group, and 35.2% ± 5.5 in the BoNT-A group [$P = 0.40$]) (**Fig. 8B**). The duration of dural arterial dilation was not significantly different between treatment groups, about 2210 ± 220 seconds in saline and 2600 ± 190 seconds in BoNT-A ($P = 0.20$), as well as the area under the curve, 129 ± 1.7 for saline and 129 ± 2.9 for BoNT-A ($P = 0.94$). There was no significant interaction between treatment group and time post-CSD according to a two-way ANOVA, ($F_{(44,1)} = 1.1$, $P = 0.39$). Pial veins were also not significantly different between treatment groups in regards to initial pial vein maximal dilation (11.9% ± 2.1 saline, 10.1% ± 1.8 BoNT-A, $P = 0.52$) or duration (997 seconds ± 250 saline, 832 seconds ± 300 BoNT-A, $P = 0.68$), secondary pial vein dilation maximum (19.2% ± 3.2 saline, 16.7% ± 4.2 BoNT-A, $P = 0.64$), duration (2110 seconds ± 400 saline, 2040 s ± 380 BoNT-A, $P = 0.90$), or area under the curve (54.1 ± 1.4 saline, 54.7 ± 1.5 BoNT-A, $P = 0.78$) (**Fig. 8C**). A repeated measures ANOVA showed no significant interaction between treatment groups ($F_{(44,1)} = 0.34$, $P = 1.0$). Dura veins continued to show no significant changes due to CSD, and this was not affected by treatment (repeated measures ANOVA $F_{(44,1)} = 0.51$, $P = 1.0$) (**Fig. 8D**).

4. Discussion

Using standard electrocorticogram recording techniques, immunohistochemistry, and 2-photon microscopy, we report (1) that scalp but not lumbar injections of BoNT-A shorten the period of profound depression of spontaneous cortical activity that follows a pinprick-induced CSD, (2) that neither scalp nor lumbar injections prevent the induction, occurrence, propagation, or spreading velocity of a single wave of CSD, (3) that cleaved SNAP25—currently, one of the most convincing tools to determine the anatomical targeting of BoNT-A treatment—could easily be detected in the extracranial muscles where it was injected and in nerve fibers of the intracranial dura, but not in any cortical area affected by the CSD, (4) that the absence of BoNT/A-cleaved SNAP25 in the cortex is unrelated to the state of the BBB (ie, whether it is intact or compromised), (5) that BoNT-A does not alter the vascular responses to CSD, and (6) that BoNT-A effects on CSD are similar in males and females. To the best of our knowledge, this is the first report of peripherally applied BoNT-A's ability to alter neural function along any CNS pathway involved in the pathophysiology of migraine. Adhering to evidence-based reasoning, we interpret the presence of cleaved SNAP25 in dural nerve fibers and the unequivocal absence of cleaved SNAP25 in the cortex as suggesting that the shortening of the cortical recovery period that follows CSD, does not involve a direct action of BoNT-A or the transport of cleaved SNAP25 from the periphery to the cortex. Instead, we propose that it must be mediated by a yet-unknown "indirect" effect from a local action of the neurotoxin on extracranial and intracranial tissues outside the BBB. Mechanistically, these findings suggest (1) that different physiological mechanisms govern CSD's amplitude, propagation, and the cortical depression that follows and (2) that the cleaved SNAP25 we observed in dural nerve fibers after scalp/suture-line injections of BoNT-A—a novel finding on its own—does not seem to regulate secretion of molecules that facilitate dilatation or constriction of pial or dural arteries or veins in response to CSD. Therapeutically, the findings raise the possibility that at least some aspects of BoNT-A's ability to reduce occurrence of migraine may involve lessening the overall impact of CSD on the activation of meningeal nociceptors, and that gender is unlikely to play a role in BoNT-A efficacy.

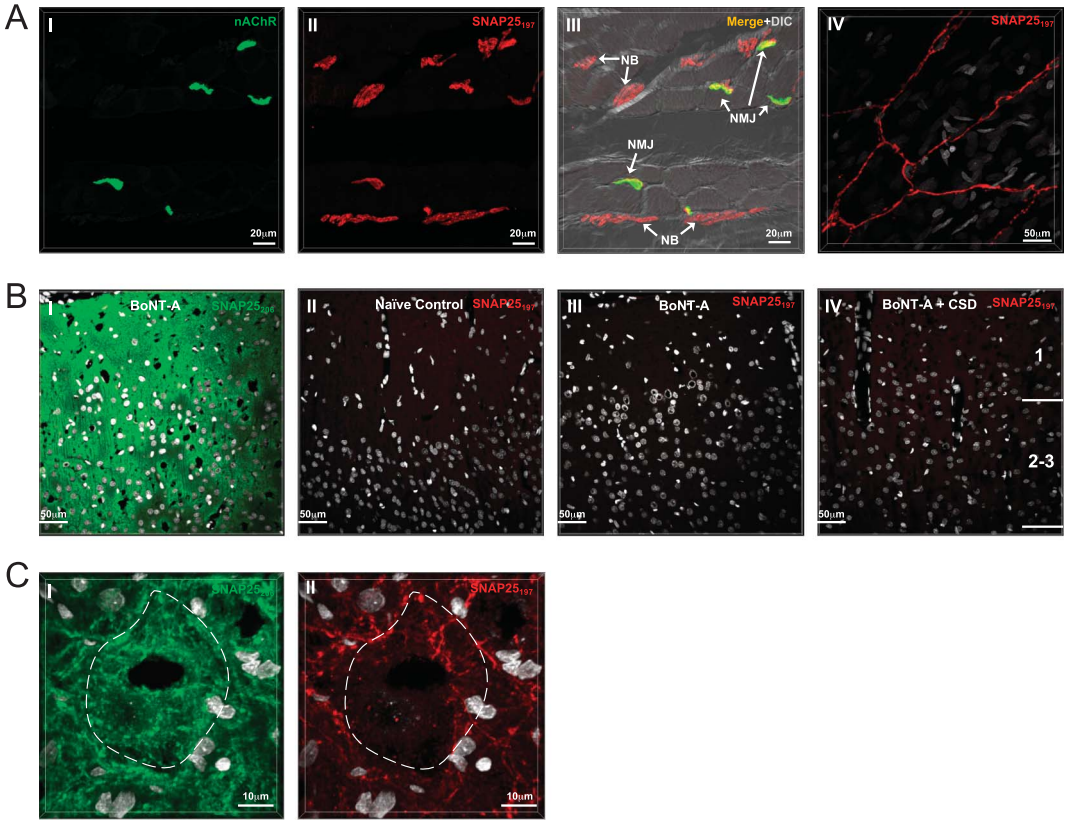

Figure 7. Presence and absence of SNAP25 ($SNAP25_{206}$) and BoNT-A-cleaved SNAP25 ($SNAP25_{197}$) in muscles, dura, visual cortex, and spinal cord after scalp injections of BoNT-A. (A) Confocal images of rat temporal muscle and intracranial dura taken 7 days after BoNT-A injections. (I) Nicotinic acetylcholine receptors (nAChR) labeled by α-bungarotoxin Alexa Fluor 488. (II) Immunostaining for $SNAP25_{197}$. (III) Merge of the staining in I and II on a muscle fiber background imaged by differential interference contrast optics (Merge + differential interference contrast). (IV) Confocal image of whole-mount rat dura showing $SNAP25_{197}$-positive nerve fibers. (B) Confocal images of the visual cortex taken from the group that received scalp/suture-line injections of BoNT-A 7 days earlier. (I) Presence of uncleaved SNAP25 ($SNAP25_{206}$/green) in rats with intact BBB. (II) Absence of cleaved SNAP25 ($SNAP25_{197}$/red) in naive (uninjected) rats. (III) Absence of cleaved SNAP25 ($SNAP25_{197}$/red) in BoNT-A-injected rats with intact BBB ($SNAP25_{197}$/red). (IV) Absence of cleaved SNAP25 ($SNAP25_{197}$/red) in BoNT-A-injected rats with compromised BBB ($SNAP25_{197}$/red). DAPI-labeled cell nuclei are shown in gray (I-IV), and cortical layers are delineated in IV. (C) Central nervous system detection of cleaved SNAP25. High-magnification confocal images of an individual, 3D-reconstructed motor neuron in the ventrolateral spinal cord, one week after BoNT-A injections (30 U/kg) into lower-limb muscles. Note staining of uncleaved (I) and cleaved (II) SNAP25. BBB, blood–brain barrier; BoNT-A, onabotulinumtoxinA; NB, axon nerve bundle; NMJ, neuromuscular junction.

Clinically, the most relevant finding of this study is that neither induction nor occurrence, propagation, or spreading velocity of a single wave of CSD was affected by scalp/suture-line injections of BoNT-A. It is clinically relevant because it suggests that successful migraine prophylaxis can be achieved by a peripherally acting drug that may lack the ability to prevent aura. Although the findings of this preclinical study support this conclusion and provide a plausible mechanistic explanation (ie, lack of cleaved SNAP25 in the cortex after BoNT-A injections), it must be acknowledged that their translation into clinical relevance is currently less obvious for lack of high-quality studies on the occurrence of aura after BoNT-A treatment in patients with migraine with aura who benefit from this treatment as well as those who do not. Along this line, it will also be informative to determine the incidence of *delayed-onset prevention of aura* in treatment responders (ie, in those in which BoNT-A treatment reduces the number of migraine days per month by >50%), as such finding can support an "indirect" effect that is secondary to BoNT-A's ability to provide patients with a prolonged period of no headache, which is likely to attenuate the overall excitability of the cortex because of reduced or elimination of its continuous bombardment with pain signals.

Preclinically, the finding that BoNT-A treatment did not slow down the propagation rate of CSD is worthwhile noting because it is the only migraine preventive drug not doing so. To date, all tested centrally (ie, amitriptyline, valproate, propranolol, propofol, topiramate, gabapentin, methysergide, lamotrigine, tonabersat, and ketamine) and peripherally (fremanezumab) acting migraine preventive drugs seem to slow down the propagation rate of CSD.[3,4,11,18,21,32,43,48] If, as suggested, slowing the propagation rate of CSD in animal studies is relevant to a drug's ability to prevent migraine,[3] the current study suggests that the mechanism by which BoNT-A prevents migraine differ from the mechanism by which all other migraine preventive drugs work. But before adopting this notion, we must recognize the gap in our understanding of what exactly determines the velocity at which neuronal depolarization spreads.[13] What may be relevant to this discussion is the fact that some of the better studied ionic and molecular events may be independent of the SNARE-mediated synaptic release mechanism (eg, increased intracellular Ca2+, decreased Ca2+ influx, massive K+ release, and its rapid clearance from the interstitial fluid),[38,40,47] whereas others may depend on it (eg, the large glutamate release and its clearance from the interstitial fluid,[14,45]).

By far, the most unexpected finding in this study is that the profound depression of spontaneous and evoked cortical activity, which is one of the most notable characteristics of spreading depolarization,[26,47] was significantly shorter in rats in which BoNT-A

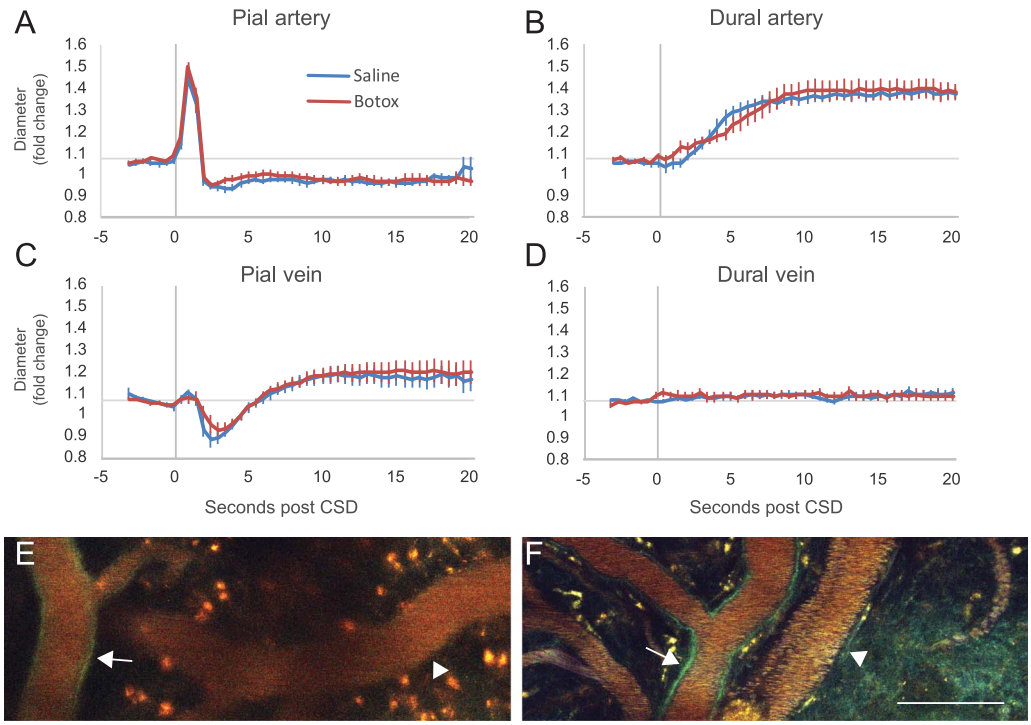

Figure 8. OnabotulinumtoxinA does not alter vascular responses to CSD. Plots of the average fold change in pial arteries (A), dural arteries (B), pial veins (C), and dural veins (D) during CSD in BoNT-A (n = 10) and saline (n = 10)-injected rats. In vivo images of arteries (arrows) and veins (arrowheads) in the pia (E) and dura (F) taken with a wavelength of 800 nm, which reveals smooth muscle as a green border around arteries. BoNT-A, onabotulinumtoxinA; CSD, cortical spreading depression.

was injected in the scalp muscles and suture line, but not in the lumbar region. We interpret these findings as suggesting that the shortening of the neuronal silencing period is achieved primarily through a localized action of the neurotoxin in cranial tissues. In building on this line of reasoning, we took into consideration the finding that 7 days after extracranial BoNT-A injections (ie, along the suture lines) cleaved SNAP25 was found in multiple dural nerve fibers *but not in any of the examined cortical areas involved in the CSD*. In the absence of data that can explain how inhibition of unmyelinated nerve fibers in the dura and potentially their branches in the pia[22]—where they have close relationship with the cerebral cortex—can shorten the cortical silencing period that follows the CSD, we can only speculate that reduced release of neuropeptides, neurotransmitters, and/or other signaling molecules (eg, CGRP, pituitary adenylate cyclase-activating polypeptide, somatostatin, galanin, substance P, cholecystokinin, glutamate, vasoactive intestinal peptide, neuropeptide Y, nociception, ATP, nitric oxide, and cytokines[15,25,35]) from trigeminal axons that reach the pia may play a role in it. Regardless of our current lack of evidence-based explanation for the BoNT-A's ability to shorten the recovery period of the cortex, these findings emphasize the view that the therapeutic effects of most migraine (and probably nonmigraine analgesics) drugs are likely to involve multiple mechanisms at multiple sites.

More broadly, the presence of cleaved SNAP25 in multiple dural nerve fibers provides a much needed anatomical/mechanistic explanation for how extracranial injections of BoNT-A block or reduce activation of intracranial unmyelinated nerve fibers in the dura.[7,34,53] Given all the evidence for the role played by meningeal nociceptors in the initiation, and potentially maintenance of the headache phase of migraine, these anatomical findings may strengthen the view that the therapeutic effects of BoNT-A in migraine prophylaxis involve direct interaction with and inhibition of meningeal pain fibers.[7,34,53] Inhibitory effects of BoNT-A on peripheral nociceptors may also explain its therapeutic effects in the treatment of chronic neuropathic pain.[1,41]

Conflict of interest statement

The authors have no conflicts of interest to declare.

Allergan, an AbbVie company, holds the patent for treating chronic migraine with onabotulinumtoxinA. Allergan funded parts of the study. R.S. Broide, B.B. Cai, C. Rhéaume, A.D. Brideau-Andersen, and M.F. Brin are employees of Allergan, and R. Burstein is a consultant to Allergan.

Acknowledgements

This study was funded by a grant from Allergan and NIH grants NS079678, NS094198, and NS106345 to R. Burstein and A.M. Strassman.

Article history:
Received 20 December 2020
Received in revised form 11 January 2021
Accepted 1 February 2021
Available online 16 March 2021

References

[1] Attal N, de Andrade DC, Adam F, Ranoux D, Teixeira MJ, Galhardoni R, Raicher I, Uceyler N, Sommer C, Bouhassira D. Safety and efficacy of repeated injections of botulinum toxin A in peripheral neuropathic pain (BOTNEP): a randomised, double-blind, placebo-controlled trial. Lancet Neurol 2016;15:555–65.

[2] Aurora SK, Dodick DW, Turkel CC, DeGryse RE, Silberstein SD, Lipton RB, Diener HC, Brin MF. OnabotulinumtoxinA for treatment of chronic

migraine: results from the double-blind, randomized, placebo-controlled phase of the PREEMPT 1 trial. Cephalalgia 2010;30:793–803.
[3] Ayata C, Jin H, Kudo C, Dalkara T, Moskowitz MA. Suppression of cortical spreading depression in migraine prophylaxis. Ann Neurol 2006;59:652–61.
[4] Bogdanov VB, Multon S, Chauvel V, Bogdanova OV, Prodanov D, Makarchuk MY, Schoenen J. Migraine preventive drugs differentially affect cortical spreading depression in rat. Neurobiol Dis 2011;41:430–5.
[5] Brennan KC, Pietrobon D. A systems neuroscience approach to migraine. Neuron 2018;97:1004–21.
[6] Burstein R, Jakubowski M. Analgesic triptan action in an animal model of intracranial pain: a race against the development of central sensitization. Ann Neurol 2004;55:27–36.
[7] Burstein R, Zhang X, Levy D, Aoki KR, Brin MF. Selective inhibition of meningeal nociceptors by botulinum neurotoxin type A: therapeutic implications for migraine and other pains. Cephalalgia 2014;34:853–69.
[8] Cai BB, Francis J, Brin MF, Broide RS. Botulinum neurotoxin type A-cleaved SNAP25 is confined to primary motor neurons and localized on the plasma membrane following intramuscular toxin injection. Neuroscience 2017;352:155–69.
[9] Charles A. Migraine: a brain state. Curr Opin Neurol 2013;26:235–9.
[10] Cutrer FM, Sorensen AG, Weisskoff RM, Ostergaard L, Sanchez del Rio M, Lee EJ, Rosen BR, Moskowitz MA. Perfusion-weighted imaging defects during spontaneous migrainous aura. Ann Neurol 1998;43: 25–31.
[11] Dhir A, Lossin C, Rogawski MA. Propofol hemisuccinate suppresses cortical spreading depression. Neurosci Lett 2012;514:67–70.
[12] Diener HC, Dodick DW, Aurora SK, Turkel CC, DeGryse RE, Lipton RB, Silberstein SD, Brin MF. OnabotulinumtoxinA for treatment of chronic migraine: results from the double-blind, randomized, placebo-controlled phase of the PREEMPT 2 trial. Cephalalgia 2010;30:804–14.
[13] Enger R, Tang W, Vindedal GF, Jensen V, Johannes Helm P, Sprengel R, Looger LL, Nagelhus EA. Dynamics of ionic shifts in cortical spreading depression. Cereb Cortex 2015;25:4469–76.
[14] Fabricius M, Jensen LH, Lauritzen M. Microdialysis of interstitial amino acids during spreading depression and anoxic depolarization in rat neocortex. Brain Res 1993;612:61–9.
[15] Goto T, Iwai H, Kuramoto E, Yamanaka A. Neuropeptides and ATP signaling in the trigeminal ganglion. Jpn Dent Sci Rev 2017;53:117–24.
[16] Hadjikhani N, Sanchez Del Rio M, Wu O, Schwartz D, Bakker D, Fischl B, Kwong KK, Cutrer FM, Rosen BR, Tootell RB, Sorensen AG, Moskowitz MA. Mechanisms of migraine aura revealed by functional MRI in human visual cortex. Proc Natl Acad Sci U S A 2001;98:4687–92.
[17] Hansen JM, Lipton RB, Dodick DW, Silberstein SD, Saper JR, Aurora SK, Goadsby PJ, Charles A. Migraine headache is present in the aura phase: a prospective study. Neurology 2012;79:2044–9.
[18] Hoffmann U, Dilekoz E, Kudo C, Ayata C. Gabapentin suppresses cortical spreading depression susceptibility. J Cereb Blood Flow Metab 2010;30: 1588–92.
[19] Jakubowski M, Levy D, Goor-Aryeh I, Collins B, Bajwa Z, Burstein R. Terminating migraine with allodynia and ongoing central sensitization using parenteral administration of COX1/COX2 inhibitors. Headache 2005;45:850–61.
[20] Jakubowski M, Levy D, Kainz V, Zhang XC, Kosaras B, Burstein R. Sensitization of central trigeminovascular neurons: blockade by intravenous naproxen infusion. Neuroscience 2007;148:573–83.
[21] Kazemi H, Rahgozar M, Speckmann EJ, Gorji A. Effect of cannabinoid receptor activation on spreading depression. Iran J Basic Med Sci 2012; 15:926–36.
[22] Kosaras B, Jakubowski M, Kainz V, Burstein R. Sensory innervation of the calvarial bones of the mouse. J Comp Neurol 2009;515:331–48.
[23] Lauritzen M. Pathophysiology of the migraine aura. The spreading depression theory. Brain 1994;117(pt 1):199–210.
[24] Lauritzen M, Dreier JP, Fabricius M, Hartings JA, Graf R, Strong AJ. Clinical relevance of cortical spreading depression in neurological disorders: migraine, malignant stroke, subarachnoid and intracranial hemorrhage, and traumatic brain injury. J Cereb Blood Flow Metab 2011;31:17–35.
[25] Lazarov NE. Comparative analysis of the chemical neuroanatomy of the mammalian trigeminal ganglion and mesencephalic trigeminal nucleus. Prog Neurobiol 2002;66:19–59.
[26] Leao A. Spreading depression of activity in cerebral cortex. J Neurophysiol 1944;7:359–90.
[27] Leao AA. Further observations on the spreading depression of activity in the cerebral cortex. J Neurophysiol 1947;10:409–14.
[28] Leao AA. Spreading depression. Funct Neurol 1986;1:363–6.
[29] Levy D, Jakubowski M, Burstein R. Disruption of communication between peripheral and central trigeminovascular neurons mediates the antimigraine action of 5HT 1B/1D receptor agonists. Proc Natl Acad Sci U S A 2004;101:4274–9.
[30] Levy D, Zhang XC, Jakubowski M, Burstein R. Sensitization of meningeal nociceptors: inhibition by naproxen. Eur J Neurosci 2008;27:917–22.
[31] Melo-Carrillo A, Noseda R, Nir RR, Schain AJ, Stratton J, Strassman AM, Burstein R. Selective inhibition of trigeminovascular neurons by fremanezumab: a humanized monoclonal anti-CGRP antibody. J Neurosci 2017;37:7149–63.
[32] Melo-Carrillo A, Schain AJ, Stratton J, Strassman AM, Burstein R. Fremanezumab and its isotype slow propagation rate and shorten cortical recovery period but do not prevent occurrence of cortical spreading depression in rats with compromised blood-brain barrier. PAIN 2020; 161:1037–43.
[33] Melo-Carrillo A, Strassman AM, Nir RR, Schain AJ, Noseda R, Stratton J, Burstein R. Fremanezumab-A humanized monoclonal anti-CGRP antibody-inhibits thinly myelinated (adelta) but not unmyelinated (C) meningeal nociceptors. J Neurosci 2017;37:10587–96.
[34] Melo-Carrillo A, Strassman AM, Schain AJ, Noseda R, Ashina S, Adams A, Brin MF, Burstein R. Exploring the effects of extracranial injections of botulinum toxin type A on prolonged intracranial meningeal nociceptors responses to cortical spreading depression in female rats. Cephalalgia 2019;39:1358–65.
[35] Messlinger K, Balcziak LK, Russo AF. Cross-talk signaling in the trigeminal ganglion: role of neuropeptides and other mediators. J Neural Transm (Vienna) 2020;127:431–44.
[36] Milner PM. Note on a possible correspondence between the scotomas of migraine and spreading depression of Leao. Electroencephalogr Clin Neurophysiol 1958;10:705.
[37] Moskowitz MA, Macfarlane R. Neurovascular and molecular mechanisms in migraine headaches. Cerebrovasc Brain Metab Rev 1993;5:159–77.
[38] Newman EA. High potassium conductance in astrocyte endfeet. Science 1986;233:453–4.
[39] Noseda R, Schain AJ, Melo-Carrillo A, Tien J, Stratton J, Mai F, Strassman AM, Burstein R. Fluorescently-labeled fremanezumab is distributed to sensory and autonomic ganglia and the dura but not to the brain of rats with uncompromised blood brain barrier. Cephalalgia 2020;40:229–40.
[40] Pietrobon D, Moskowitz MA. Chaos and commotion in the wake of cortical spreading depression and spreading depolarizations. Nat Rev Neurosci 2014;15:379–93.
[41] Ranoux D, Attal N, Morain F, Bouhassira D. Botulinum toxin type A induces direct analgesic effects in chronic neuropathic pain. Ann Neurol 2008;64:274–83.
[42] Rasmussen BK, Olesen J. Migraine with aura and migraine without aura: an epidemiological study. Cephalalgia 1992;12:221–8; discussion 186.
[43] Read SJ, Hirst WD, Upton N, Parsons AA. Cortical spreading depression produces increased cGMP levels in cortex and brain stem that is inhibited by tonabersat (SB-220453) but not sumatriptan. Brain Res 2001;891:69–77.
[44] Rheaume C, Cai BB, Wang J, Fernandez-Salas E, Aoki KR, Francis J, Broide RS. A highly specific monoclonal antibody for botulinum neurotoxin type A-cleaved SNAP25. Toxins (Basel) 2015;7:2354–70.
[45] Rimmele TS, de Castro Abrantes H, Wellbourne-Wood J, Lengacher S, Chatton JY. Extracellular potassium and glutamate interact to modulate mitochondria in astrocytes. ACS Chem Neurosci 2018;9:2009–15.
[46] Sanchez del Rio M, Bakker D, Wu O, Agosti R, Mitsikostas DD, Ostergaard L, Wells WA, Rosen BR, Sorensen G, Moskowitz MA, Cutrer FM. Perfusion weighted imaging during migraine: spontaneous visual aura and headache. Cephalalgia 1999;19:701–7.
[47] Somjen GG. Mechanisms of spreading depression and hypoxic spreading depression-like depolarization. Physiol Rev 2001;81:1065–96.
[48] Unekawa M, Tomita Y, Toriumi H, Suzuki N. Suppressive effect of chronic peroral topiramate on potassium-induced cortical spreading depression in rats. Cephalalgia 2012;32:518–27.
[49] Viana M, Sances G, Linde M, Ghiotto N, Guaschino E, Allena M, Terrazzino S, Nappi G, Goadsby PJ, Tassorelli C. Clinical features of migraine aura: results from a prospective diary-aided study. Cephalalgia 2017;37:979–89.
[50] Viana M, Tronvik EA, Do TP, Zecca C, Hougaard A. Clinical features of visual migraine aura: a systematic review. J Headache Pain 2019;20:64.
[51] Zhang X, Levy D, Kainz V, Noseda R, Jakubowski M, Burstein R. Activation of central trigeminovascular neurons by cortical spreading depression. Ann Neurol 2011;69:855–65.
[52] Zhang X, Levy D, Noseda R, Kainz V, Jakubowski M, Burstein R. Activation of meningeal nociceptors by cortical spreading depression: implications for migraine with aura. J Neurosci 2010;30:8807–14.
[53] Zhang X, Strassman AM, Novack V, Brin MF, Burstein R. Extracranial injections of botulinum neurotoxin type A inhibit intracranial meningeal nociceptors' responses to stimulation of TRPV1 and TRPA1 channels: are we getting closer to solving this puzzle?. Cephalalgia 2016;36: 875–86.